Loss of heme oxygenase-1 accelerates mesodermal gene expressions during embryoid body development from mouse embryonic stem cells

Yan-Liang Lai[a,b,1], Chen-Yu Lin[a,1], Wei-Cheng Jiang[a,1], Yen-Chun Ho[a], Chung-Huang Chen[a], Shaw-Fang Yet[a,c,*]

[a] Institute of Cellular and System Medicine, National Health Research Institutes, Zhunan, Taiwan
[b] Institute of Molecular Medicine, National Tsing Hua University, Hsinchu, Taiwan
[c] Graduate Institute of Biomedical Sciences, China Medical University , Taichung, Taiwan

ARTICLE INFO

ABSTRACT

Heme oxygenase (HO)-1 is an inducible stress response protein and well known to protect cells and tissues against injury. Despite its important function in cytoprotection against physiological stress, the role of HO-1 in embryonic stem cell (ESC) differentiation remains largely unknown. We showed previously that induced pluripotent stem (iPS) cells that lack HO-1 are more sensitive to oxidant stress-induced cell death and more prone to lose pluripotent markers upon LIF withdrawal. To elucidate the role of HO-1 in ESC differentiation and to rule out the controversy of potential gene flaws in iPS cells, we derived and established mouse HO-1 knockout ESC lines from HO-1 knockout blastocysts. Using wild type D3 and HO-1 knockout ESCs in the 3-dimensional embryoid body (EB) differentiation model, we showed that at an early time point during EB development, an absence of HO-1 led to enhanced ROS level, concomitant with increased expressions of master mesodermal regulator brachyury and endodermal marker GATA6. In addition, critical smooth muscle cell (SMC) transcription factor serum response factor and its coactivator myocardin were enhanced. Furthermore, HO-1 deficiency increased Smad2 in ESCs and EBs, revealing a role of HO-1 in controlling Smad2 level. Smad2 not only mediates mesendoderm differentiation of mouse ESCs but also SMC development. Collectively, loss of HO-1 resulted in higher level of mesodermal and SMC regulators, leading to accelerated and enhanced SMC marker SM α-actin expression. Our results reveal a previously unrecognized function of HO-1 in regulating SMC gene expressions during ESC-EB development. More importantly, our findings may provide a novel strategy in enhancing ESC differentiation toward SMC lineage.

1. Introduction

Heme oxygenase (HO) family of proteins includes HO-1, HO-2, and HO-3. HO catalyzes the oxidation of heme to generate carbon monoxide (CO), biliverdin, and ferrous iron [1]. Ferrous iron can induce ferritin expression for iron sequestration while biliverdin is subsequently reduced by biliverdin reductase to bilirubin, a potent endogenous antioxidant [2,3]. CO has many biological functions including suppression of oxidative stress and inflammation [4,5]. Of the HO isoforms, HO-1 is inducible whereas HO-2 constitutive and HO-3 less characterized. HO-1 is of particular interest because it is a stress response protein. HO-1 is expressed at low levels under basal physiological conditions; however, in response to various pathological stresses, HO-1 is upregulated to serve an endogenous protective, defense mechanism [6–8]. We and others have shown that HO-1 protects heart from myocardial injury

[9–13] whereas in blood vessels, HO-1 protects against various vascular diseases such as atherosclerosis, restenosis, and aortic aneurysm [14–17]. Numerous studies have now established a critical protective function of HO-1 in the cardiovascular and other organ systems [7,18–21]. Highlighting the crucial physiological role of HO-1 against various oxidative stresses and inflammation in the human body, there are only two cases of human HO-1 deficiency identified to date and both patients died at a young age of 6 and 15, respectively [22–25]. The mother of the 6 years old boy had experienced 2 intrauterine fetal deaths [23], suggesting a critical function of HO-1 in embryonic development.

In addition to protecting against tissue injury, HO-1 has been implicated a role in postnatal differentiation [26]. For example, HO-1-derived CO induces erythroid differentiation of K562 cells [27], and permits maturation of myeloid cells [28]. Bone marrow-derived

mesenchymal stem cells (MSCs) can differentiate into many different cell types, including adipocytes and osteoblasts. In MSCs, increased expression of HO-1 shifts the balance of differentiation towards osteoblast lineage; in contrast, a decrease in HO-1 drives MSCs toward adipogenesis [29]. Supporting this notion, HO-1 inhibits preadipocyte proliferation and differentiation at the onset of obesity [30]. Taken together, these studies indicate a role of HO-1 in postnatal differentiation in various cell types.

In view of HO-1 knockout mice were born less than predicted Mendelian distribution [9,31] and the rare cases of human HO-1 deficiency, HO-1 might have a critical role in embryonic stem cell (ESC) biology, differentiation, and development. Furthermore, it is well recognized that redox homeostasis regulates stem cell renewal and differentiation [32]. ESCs are characterized by low reactive oxygen species (ROS) level and a low capacity to remove extracellular hydrogen peroxide, assessed by a quantitative redox biology approach [33]. During cardiomyocyte differentiation from ESCs, ROS levels are increased [34]. In addition, multiple stress defense mechanisms are downregulated during ESC differentiation [35]. The collective information indicates a crucial role of redox status in ESC differentiation. HO-1 is expressed in undifferentiated human ESCs and is involved in suppressing the allogenic proliferative response of lymphocytes, suggesting involvement of HO-1 in protecting ESCs [36]. To investigate functional role of HO-1 in ESCs, we have previously generated induced pluripotent stem (iPS) cells of HO-1$^{+/+}$, HO-1$^{+/-}$, and HO-1$^{-/-}$ genotypes from mouse embryonic fibroblasts [37]. Consistent with human ESCs, HO-1 is expressed in wild type D3 ESCs and iPS-HO-1$^{+/+}$ cells. Compared with mouse D3 ESCs or iPS-HO-1$^{+/+}$ cells, iPS-HO-1$^{-/-}$ cells are more prone to oxidant stress-induced cell death. In addition, during spontaneous differentiation on a monolayer, lack of HO-1 leads to an accelerated reduction of pluripotent marker Oct4 expression [37].

Although we have shown that lack of HO-1 accelerates loss of pluripotency in iPS-HO-1$^{-/-}$ cells [37], the effect of HO-1 on differentiation was not addressed. The goal of this study was to elucidate the role of HO-1 in ESC differentiation. To this end and to rule out the controversy of potential gene flaws in iPS cells [38,39], we derived and established mouse HO-1$^{-/-}$ ESC lines from HO-1$^{-/-}$ blastocysts for the experiments. Here we showed that loss of HO-1 enhanced ROS level at an early time point during embryoid body (EB) development, concomitant with elevated levels of mesendodermal and smooth muscle cell (SMC) transcriptional regulators. Importantly, Smad2, which mediates Activin/Nodal signaling in mesendoderm differentiation of mouse ESCs, was elevated in HO-1$^{-/-}$ ESCs and EBs. The concerted elevations of these regulators in the absence of HO-1 might orchestrate the accelerated and enhanced expression of SMC marker smooth muscle (SM) α-actin expression. Our results demonstrate a critical role of HO-1 during ESC differentiation in modulating SMC gene expressions.

2. Materials and methods

2.1. ESC culture and in vitro spontaneous differentiation

Mouse ESCs were cultured on mitomycin C (Sigma)-inactivated mouse embryonic fibroblast feeders [37] in ESC medium (DMEM containing 15% FBS (HyClone), 3.7 g/L sodium bicarbonate, 1.7 mmol/L ʟ-glutamine, 0.1 mmol/L nonessential amino acids, 0.1 mmol/L β-mercaptoethenol, 1000 U/mL leukemia inhibitor factor (LIF; Millipore), 100 U/mL penicillin, and 100 µg/mL streptomycin). All culture reagents were from Invitrogen unless stated otherwise. For spontaneous differentiation on a monolayer, D3 wild type ESCs were plated on CellBIND culture dishes (Corning) without feeder in ESC medium omitting LIF [37]. Total proteins were then prepared at different time points after plating to detect HO-1 (Enzo Life Sciences, ADI-OSA-110) and HO-2 (Enzo Life Sciences, ADI-OSA-200) expressions by Western blot analysis as previously described [37]. To measure ROS levels during spontaneous differentiation on a monolayer, D3 ESCs were

plated and cultured as described above on 96-well CellBIND culture plates (2×10^4 cells/well). Cells at different time points after plating were harvested, suspended in PBS, and incubated with 20 µM carboxy-H2DCFDA (Thermo Fisher Scientific, C400) for 30 min at 37 °C. Cells were then washed twice with PBS to remove excess dye. The intracellular ROS accumulation was assessed by measuring DCF fluorescence using Plate CHAMELEON microplate reader (Hidex) with excitation at 485 nm and emission at 535 nm.

2.2. Derivation and characterization of HO-1$^{-/-}$ mouse ESCs

Two HO-1$^{-/-}$ mouse ESC lines were derived and established from 3.5 days postcoitum blastocysts obtained through intercrossing of HO-1 mice [9,37] using a highly efficient method [40] at the Animal Technology Institute Taiwan. Genotypes of ESC lines were determined by PCR [41] using ESC DNA samples. Karyotypes were determined at the Department of Genomic Medicine, Changhua Christian Hospital (Taiwan). To further characterize HO-1$^{-/-}$ ESCs, total proteins were prepared and Western blotting performed to detect HO-1 and HO-2 expressions. To determine growth rate, ESC doubling time was measured as described [37]. To examine pluripotency, alkaline phosphatase activity staining was performed with the alkaline phosphatase detection kit (Millipore). To evaluate ESC marker gene expressions, immunofluorescence staining for Oct4 (Santa Cruz Biotechnology, sc-9081) and SSEA-1 (Millipore, MAB4301) was performed and nuclei counterstained with DAPI (Sigma).

2.3. Three-dimensional embryoid body differentiation

To mimic embryonic development in a three-dimensional manner, we used a hanging drop method to differentiate ESCs into EBs. Briefly, ESC colonies were dissociated into single cells and suspended in ESC medium without LIF. To induce formation of EBs, 1000 cells were plated in a 20 µL drop hanging on the lid of culture dish and cultured for 3 days. EBs were collected at day 3 and transferred to ultra-low attachment 6-well plate (Corning) containing fresh ESC medium without LIF. For further suspension culture, medium was refreshed at day 5. EBs were harvested at day 3, 5, and 7 for analysis. For Western blot analysis, total proteins were prepared from ESCs and EBs at day 3, 5, and 7 to detect expressions of HO-1, Oct4, brachyury (R&D, AF2085), SM α-actin (Sigma, A5228), SM22α (Abcam, ab155272), or Smad2 (Cell signaling, #3102). The blots were subsequently probed with α-tubulin antibody (GeneTex, GTX112141) to verify loading. To assess Erk1/2 phosphorylation, blots were probed with a rabbit anti-phospho-Erk1/2 antibody (Cell Signaling Technology, #9101) and α-tubulin antibody for loading.

2.4. RNA isolation and reverse transcription-PCR analysis

Total RNA was isolated from D3 and HO-1$^{-/-}$ ESCs and EBs with the RNeasy Mini kit (Qiagen) according to manufacturer's instructions. RNA (1 µg) was reverse transcribed to cDNA with Superscript III (Invitrogen). To first screen for potential alterations of gene expressions in 3-day EBs between D3 and HO-1$^{-/-}$, we performed PCR array to analyze 90 mouse ESC-related genes using RT^2 profiler PCR Array (Qiagen) with 3-day EB RNAs. To measure mRNA levels of 3 germ layer markers, real-time quantitative PCR was performed using 7500 real-time PCR system (Applied Biosystems) with specific primers (Table S1) to detect GATA6 (endoderm), brachyury (mesoderm), and FGF5 (ectoderm). For normalization, GAPDH was also amplified. Quantitation was performed by the comparative C_T method and the mRNA expressions normalized to GAPDH. To measure SMC gene expressions, PCR was performed with the transcribed cDNA with primer sets (Table S1) for serum response factor (SRF), myocardin, SM α-actin, and GAPDH (for normalization). The PCR products were analyzed on agarose gels and quantified using ImageJ.

2.5. Measurement of reactive oxygen species (ROS) levels in ESCs and EBs

Cellular ROS levels were measured by flow cytometry essentially as described [42]. Briefly, ESCs and EBs were dissociated into single cells with trypsin and suspended in LIF-free medium containing 20 μM carboxy-H2DCFDA and 5 μM verapamil (Sigma, V4629) for 30 min at 37 °C. Cells were then washed with PBS, resuspended in medium containing 5 μM verapamil, and analyzed in a FASCalibur flow cytometry system (BD Biosciences). The median of the gated fluorescence peak was used as an estimate of ROS levels.

2.6. Directed differentiation of adipogenesis and osteogenesis

A mouse embryonic stem cell adipogenesis kit (Millipore, SCR100) was used to direct differentiation of ESCs to adipocytes per manufacturer's instructions. Briefly, D3 and HO-1$^{-/-}$ ESC colonies were dissociated into single cells and suspended in ESC medium without LIF. To induce formation of EB, 5000 cells were plated in each drop of 15 μL hanging on the lid of culture dish and cultured for 2 days. Equal numbers of EBs (in duplicate) were then transferred to low attachment 6-well plate (Corning) in induction medium containing retinoic acid for 3 days before subjecting EBs to adipocyte differentiation medium containing T_3 and insulin. At different time points (15, 18, and 21 days) after initiating adipocyte differentiation cells were stained with Oil Red O for fat droplets in adipocytes. Cells were visualized and photographs taken before dye extraction. To quantify Oil Red O, the red dye was then extracted and absorbance read at 520 nm. For directed differentiation of ESCs toward osteoblasts, D3 and HO-1$^{-/-}$ ESCs (1000 cells/20 μL per droplet) were used to form EBs. After 3 days, EBs were dissociated into single cells with trypsin and plated as described [43] with minor modifications (1×10^4 cells/cm^2 in 12-well tissue culture dish). Cells were cultured in osteogenic differentiation medium containing 10% FBS, 50 μg/mL ascorbic acid, 10 mM β-glycerophosphate, and 5×10^{-8} M 1α,25-OH vitamin D3 [44] for 21 days. von Kossa staining with silver nitrate was then performed to detect calcium deposits [43].

2.7. Flow cytometric analysis of adipocytes and smooth muscle cells

To determine percentage differentiation of adipocytes and SMCs following EB development, cells from D3 and HO-1$^{-/-}$ 7-day EBs were subjected to flow cytometric analysis. EBs were first dissociated by Embryoid Body Dissociation kit (Miltenyi Biotec, Germany), followed by filtering through 70-μm strainers (MACS SmartStrainers) to obtain single cell suspensions. To detect adipocytes, cells were stained with Nile red as described [45]. Briefly, cells were suspended in ice-cold PBS and Nile red (Sigma, stock solution 100 μg/mL in DMSO) added to a final concentration of 0.1 μg/mL, incubated for 5 min, centrifuged, and washed once with PBS. Afterwards, cells were resuspended in an appropriate volume of PBS and kept on ice prior to flow cytometric analysis. To detect SMCs, cells were washed, fixed with 4% paraformaldehyde, permeabolized with 0.1% Triton X-100, blocked with 5% BSA, and then stained with anti-alpha smooth muscle actin antibody-FITC (Abcam, ab8211) or isotype control IgG2a-FITC (Abcam, ab18455). Acquisition was performed using FACS Calibur and cells analyzed using FlowJo software.

2.8. Rescue experiments

To chelate CO from D3 EBs, 3-day EBs were collected from the lid of culture dish, suspended in EB medium without or with hemoglobin (Sigma, H7379) (2 and 4 μM) and cultured in ultra-low attachment 6-well plate. The medium was refreshed 2 days later, cultured for 2 more days before 7-day EBs harvested. To increase ROS levels of D3 EBs, 3-day EBs were treated without or with H_2O_2 (0, 25, 50, and 100 μM) and the medium refreshed after 2 days. Total proteins were prepared from 7-day D3 EBs. To test the effect of bilirubin on HO-1$^{-/-}$ EBs, 3-day EBs

were treated with vehicle (DMSO) or various concentrations of bilirubin (Tokyo Chemical Industry) (2, 5, and 10 μM) or 1 mM N-acetylcysteine (NAC, Sigma, A9165; H_2O as a vehicle) for 2 days and total proteins prepared from 5-day EBs. To supplement CO to HO-1$^{-/-}$ EBs, 3-day EBs were suspended in EB medium containing 50 μM CO-releasing molecule tricarbonyldichlororuthenium (II) dimer (CORM2) (Sigma) or the control compound ruthenium (III) chloride (Sigma), cultured in ultra-low attachment 6-well plate for 2 days, and then proteins prepared. Western blotting was performed to detect SM α-actin. To verify loading, blots were subsequently probed with a α-tubulin antibody.

To knockdown HO-1 expression, D3 ESCs were transfected with negative control or HO-1 siRNA (Dharmacon) with Effectene reagent (Qiagen) as reported previously [37], cells were then cultured in ESC medium for 2 days before proteins isolated for Western analysis. To re-express HO-1, HO-1$^{-/-}$ ESCs were transfected with pcDNA3.1 vector or pcDNA3.1-HO-1 plasmid as reported previously [37] and cultured in ESC medium for 2 days before proteins prepared for Western blotting.

2.9. Statistical analysis

Data are presented as mean ± SE of at least three independent experiments and analyzed statistically by Student's *t*-test. *P* values < 0.05 are considered statistically significant.

3. Results

3.1. Spontaneous differentiation of ESCs on a monolayer induces HO-1 expression

To investigate the involvement of HO-1 in ESC differentiation, wild type D3 ESCs were subjected to spontaneous differentiation on a monolayer and HO-1 expression examined at different time points. Western blot analysis revealed that HO-1 was markedly induced by 3.1 ± 0.2-fold 1 day after LIF withdrawal (*P* < 0.05, n = 4) and this induction was maintained at day 2 (2.8 ± 0.2-fold; *P* < 0.05, n = 4) (Supplement Fig. S1A). Interestingly, HO-1 level quickly decreased thereafter and returned to basal levels at 3 and 4 days. In comparison, constitutively expressed isoform HO-2 did not have substantial changes (Supplement Fig. S1A). To investigate whether the induction of HO-1 was due to increased ROS during ESC differentiation, we examined ROS levels at different time points. There was a surge of ROS level at day 1 and day 2 following spontaneous differentiation (Fig. S1B). The enhanced ROS levels at day 1 and day 2 correlated with enhanced HO-1 expression. However, despite a further increase of ROS at day 3, HO-1 level had returned to basal level (Fig. S1A-B). At day 4, ROS level remained high, in contrast to basal level of HO-1 (Fig. S1A-B). Collectively, these results implicate a role of HO-1 during differentiation, particularly at early time points.

3.2. Derivation and characterization of HO-1$^{-/-}$ ESCs

To unequivocally demonstrate the important role of HO-1 in ESC differentiation, we took a loss-of-function approach by deriving and establishing two HO-1$^{-/-}$ ESC lines (9901 and 9906). The HO-1 knockout genotype of these two lines was confirmed by PCR genotyping with genomic DNA (Fig. 1A). Western blotting revealed that as with D3 wild type ESCs, HO-1$^{-/-}$ ESC lines expressed comparable levels of ESC marker gene Oct4 (Fig. 1B). As shown previously [37], compared with spleen, D3 expressed a significant level of HO-1 in ESCs (Fig. 1B). Consistent with knockout genotype, HO-1 protein was not detectable in 9901 and 9906 ESCs while HO-2 levels were similar to that of D3 ESCs (Fig. 1B). Both HO-1$^{-/-}$ ESC lines possessed strong alkaline phosphatase activity (Fig. 1C) and intense staining of ESC markers Oct4 and SSEA-1, similar to that of D3 ESCs (Fig. 1D). Karyotyping analysis showed normal karyotypes of HO-1$^{-/-}$ ESC lines (Supplement Fig. S2). Furthermore, as with a short doubling time of D3 ESCs (11.5 ± 0.8 h, n =
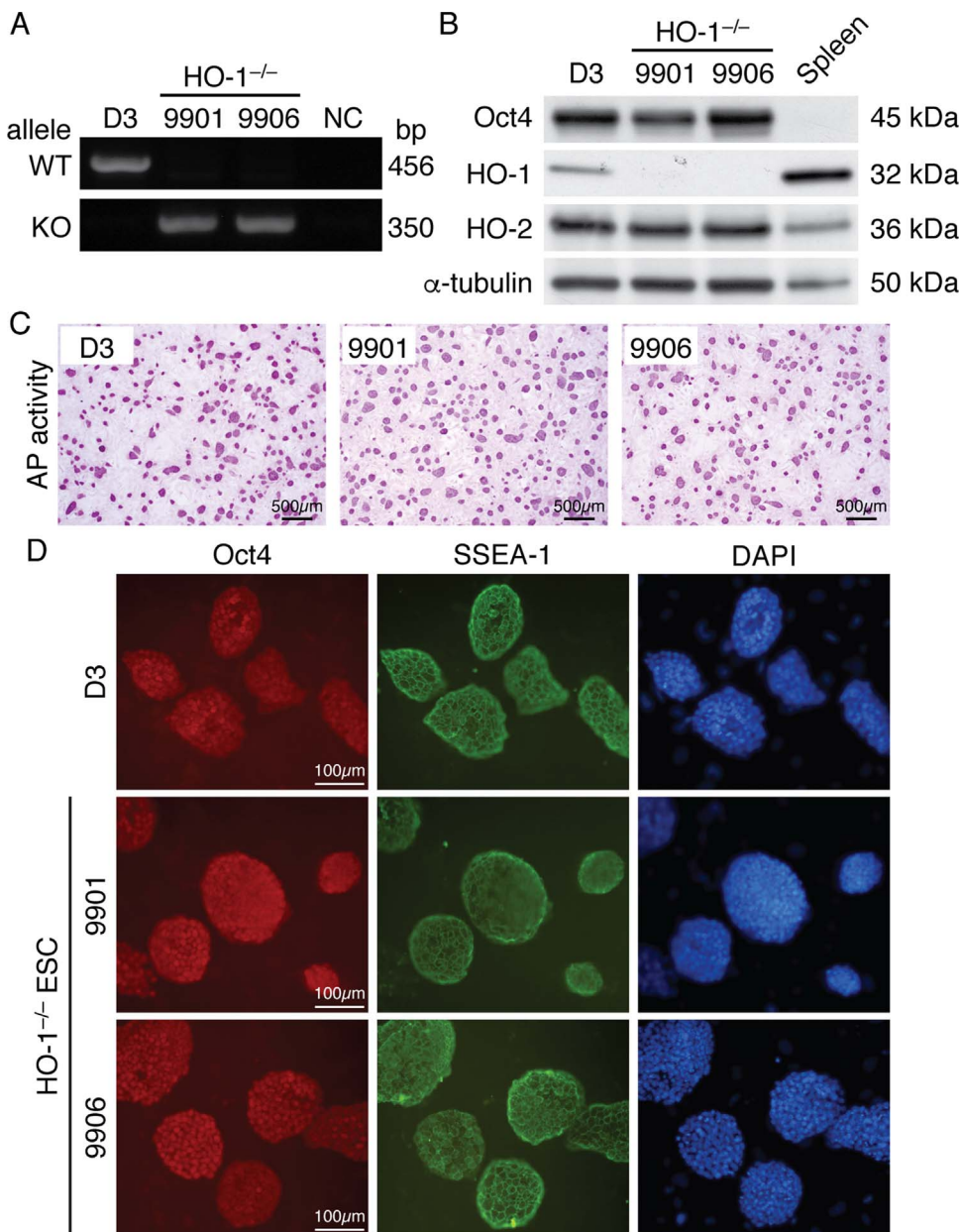
Fig. 1. *Characterization of HO-1$^{-/-}$ mouse embryonic stem cells.* Two HO-1$^{-/-}$ mouse ESC lines 9901 and 9906 were derived and characterized. (A) Genotyping was performed using PCR with genomic DNA prepared from D3, 9901, and 9906 ESCs. Water was used as a template for negative control (NC). A PCR fragment of 456-bp was amplified from wild type (WT) allele and a 350-bp fragment was amplified from knockout (KO) allele. (B) Western blot analysis was performed using total proteins prepared from D3, 9901, 9906 ESCs, and mouse spleen (for HO-1 expression control) to detect HO-1 and HO-2 expressions. To verify loading, blots were subsequently probed for α-tubulin. Protein size (kDa) is indicated at the right of the blot. (C) To examine pluripotency, alkaline phosphatase activity staining (pink) was performed. (D) For immunostaining of ESC markers, ESCs were incubated with Oct3/4 (red) and SSEA-1 (green) antibodies; nuclei were subsequently counterstained with DAPI (blue). (For interpretation of the references to color in this figure legend, the reader is referred to the web version of this article).

4), HO-1$^{-/-}$ ESC lines also had a short doubling time of 11.2 ± 0.4 h and 11.0 ± 0.4 h for 9901 and 9906, respectively (n = 4 each).

3.3. HO-1 deficiency enhances ROS levels and differentiation markers during early EB development

Embryoid bodies are primitive embryonic structures derived from differentiating ESCs and mimic embryonic development in a three-dimensional manner [46]. Given that endogenous ROS are generated during the formation of EBs and serve as signaling molecules in differentiation [34,47], we first determined whether lack of HO-1 affected ROS levels in the course of EB formation. Because the two lines of HO-1$^{-/-}$ 9901 and 9906 exhibited similar characteristics, we used one line of HO-1$^{-/-}$ ESCs (9901) for further experiments. ROS levels progressively increased in both D3 and HO-1$^{-/-}$ EBs during development (Fig. 2A). Despite that ROS levels were not different before EB formation between D3 and HO-1$^{-/-}$ ESCs, there was a significant surge of ROS levels in HO-1$^{-/-}$ EBs when compared with that of D3 at 3 days (Fig. 2A, $P < 0.05$).

Because embryonic stages equivalent to between implantation and gastrulation occur within the first two days of EB differentiation [46], we reasoned that elevated ROS at 3 days might affect HO-1$^{-/-}$ EB differentiation. We thus performed RT^2 profiler PCR array analysis using 3-day EB RNAs to screen for potential ESC-related gene alterations. Interestingly, endodermal markers (such as GATA6 and Sox17) and mesodermal marker the *T* gene (brachyury) were highly upregulated in HO-1$^{-/-}$ EBs while ectodermal marker FGF5 did not have much difference (Supplement Fig. S3). To verify this finding, we then performed quantitative Real Time-PCR (qRT-PCR) analysis of EBs at different stages from both genotypes. In comparison with D3, HO-1$^{-/-}$ EBs exhibited significantly elevated GATA6 at 3 days (16.8 ± 1.0 vs. D3 1.8 ± 0.3-fold; $P < 0.05$, n = 4) and 5 days (26.7 ± 0.3-fold vs. D3 15.2 ± 1.4-fold; $P < 0.05$, n = 4) (Fig. 2B). GATA6 was further increased at 7 days to approximately 40-fold but no significant difference was noted in both genotypes (Fig. 2B). Brachyury, which has a direct role in the early events of mesoderm formation [48,49], gradually increased during EB development in D3, 3.6 ± 0.4-fold at 3 days, 8.3 ± 1.2-fold at 5 days, and 4.4 ± 1.6-fold at 7 days (n = 3) (Fig. 2C).
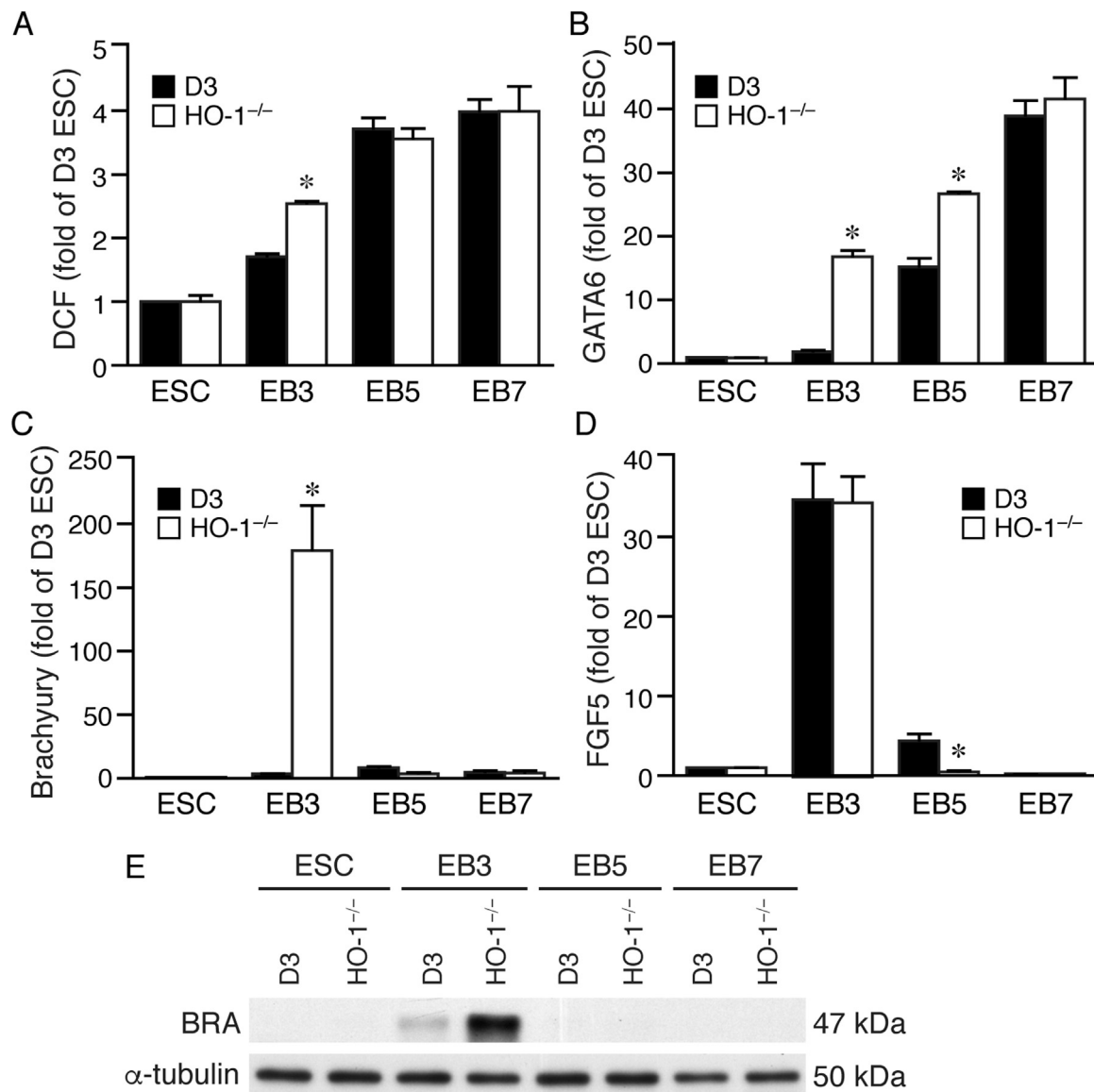
Fig. 2. *Lack of HO-1 enhances ROS levels and differentiation markers during early EB development.* (A) ROS levels were measured in ESCs and EBs at different time points by 2′,7′-di-chlorofluorescin fluorescence. Values are mean ± SE of 3 experiments. *$P < 0.05$ vs. D3. Total RNA was prepared from D3 and HO-1$^{-/-}$ ESCs and EBs at different time points and subjected to qRT-PCR analysis to measure endodermal marker GATA6 (B), mesodermal marker brachyury (C), and ectodermal marker FGF5 (D). Values are mean ± SE of at least 3–4 experiments. *$P < 0.05$ vs. D3. (E) Total proteins were isolated from ESCs and 3, 5, and 7 days after EB formation. Western blot analysis was performed to detect brachyury expression. Blots were subsequently probed with α-tubulin for normalization. A representative of 3 independent experiments is shown.

Strikingly, lack of HO-1 rendered a 179 ± 36-fold surge in 3-day HO-1$^{-/-}$ EBs (n = 3) (Fig. 2C). However, this robust induction was quickly reduced to 3.6 ± 1.3- and 4.3 ± 1.9-fold at day 5 and 7, respectively (Fig. 2C). In comparison, expression of ectodermal marker FGF5 was not different between genotypes at 3 days, although the level was lower in HO-1$^{-/-}$ than D3 EBs at 5 days (n = 4 each) (Fig. 2D). To confirm the induction pattern of brachyury at the protein level, we performed Western analysis. Brachyury protein was detectable in 3-day D3 EBs (Fig. 2E). Consistent with qRT-PCR, HO-1 deficiency resulted in a robust enhancement of brachyury proteins, compared with D3 at day 3 (Fig. 2E). Interestingly, in 5- and 7-day EBs, brachyury was barely detectable in both D3 and HO-1$^{-/-}$ EBs (Fig. 2E). The expression pattern of brachyury suggests a crucial role of HO-1 in regulating brachyury at this early time point. Together, these results indicate a critical role of HO-1 during early differentiation in regulating ROS level and germ layer differentiation, particularly endoderm and mesoderm.

3.4. Loss of HO-1 promotes adipogenesis but reduces osteogenesis in directed differentiation

In view of the robust induction of the early pan-mesoderm marker brachyury in the absence of HO-1 (Fig. 2C), we set out to investigate mesodermal differentiation potential of D3 and HO-1$^{-/-}$ ESCs in directed differentiation models. After 21 days of T_3 and insulin induction for adipogenesis, Oil Red O staining revealed many lipid-filled adipocytes derived from D3 ESCs (Fig. 3A). In comparison, substantially more red-stained adipocytes were derived from HO-1$^{-/-}$ ESCs (Fig. 3B). To assess adipogenic potential in a quantitative manner, we extracted and quantified red dye at different time points after induction. Lipid content increased in a time-dependent manner post induction (Fig. 3C). Interestingly, the lipid amount was already significantly higher in HO-1$^{-/-}$ than in D3 as early as 15 days (2.0 ± 0.1-fold, $P < 0.05$, n = 4 each) (Fig. 3C). At 18 days, although lipid accumulation in D3 increased to 1.3 ± 0.3 fold from day 15, HO-1 deficiency further augmented that to 3.5 ± 0.9-fold ($P < 0.05$, n = 4 each). Culturing in adipogenic medium
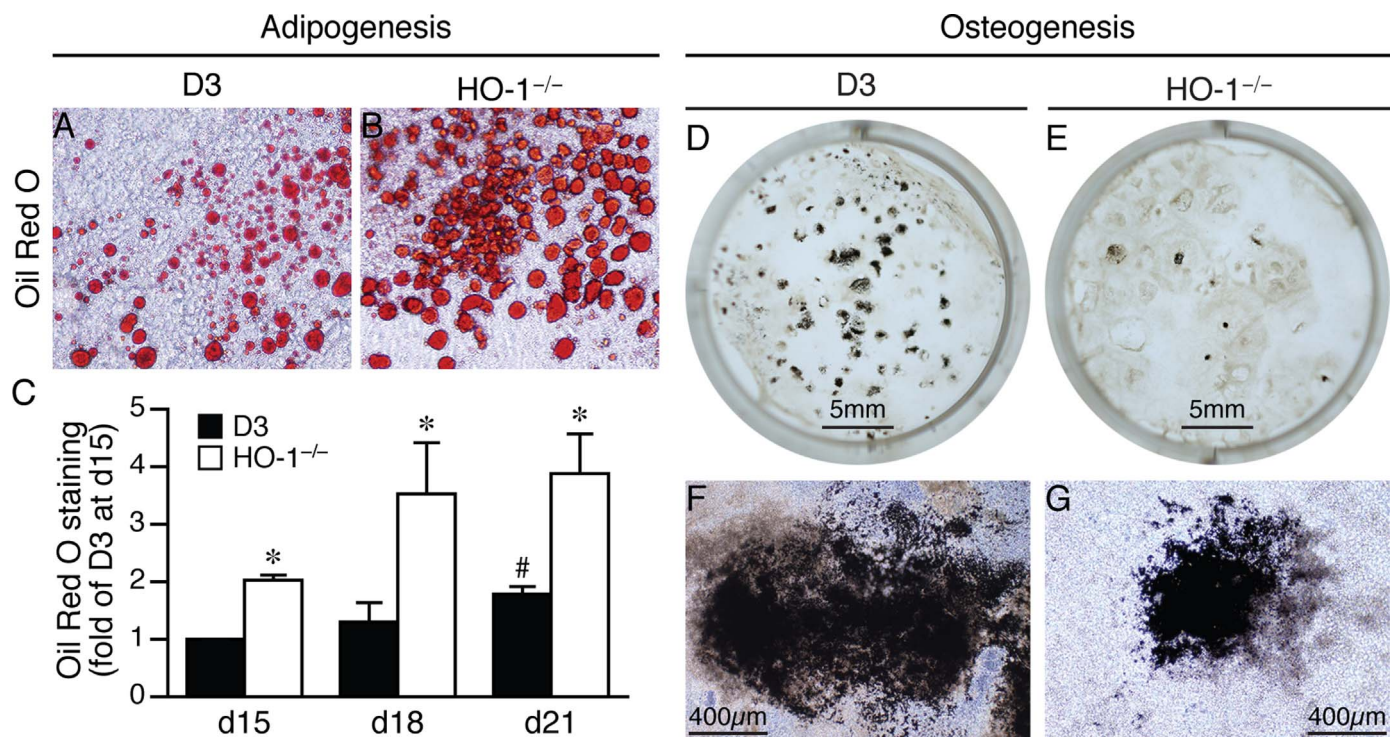
Fig. 3. *Loss of HO-1 promotes adipogenesis but reduces osteogenesis in directed differentiation.* D3 (A) and HO-1$^{-/-}$ (B) ESCs were subjected to directed differentiation of adipogenesis. Oil Red O staining was performed after 21 days for lipid-filled adipocytes (red). (C) To assess lipid accumulation at different time points in a quantitative manner, Oil Red O staining was performed 15, 18, and 21 days after differentiation, and the red dye extracted and quantified. The lipid content of D3 at 15 days was set as 1. Values are mean ± SE of 4 experiments. *$P < 0.05$ vs. D3. To assess osteogenic capacity, D3 (D) and HO-1$^{-/-}$ (E) ESCs were subjected to directed differentiation of osteogenesis. After 21 days of differentiation, von Kossa staining for calcium and phosphate minerals showed mineral deposition (black color). (E) and (G) show higher magnification of (D) and (E), respectively. (For interpretation of the references to color in this figure legend, the reader is referred to the web version of this article).

for additional 3 days (at 21 days) resulted in further lipid accumulation of D3 to 1.8 ± 0.1-fold ($P < 0.05$ vs. 15 days, n = 4 each). In comparison, lack of HO-1 significantly raised that to 3.9 ± 0.7-fold ($P < 0.05$ vs. D3, n = 4 each) (Fig. 3C), consistent with the data that more adipocytes were derived from HO-1$^{-/-}$ ESCs (Fig. 3B).

We next examined differentiation potential of ESCs toward another mesodermal lineage–osteoblasts. Twenty-one days after directed osteogenic differentiation, von Kossa staining for calcium and phosphate minerals showed plenty of mineral deposition (black color) in cells derived from D3 ESCs (Fig. 3D). In contrast with D3, mineral deposition was notably reduced in cells derived from HO-1$^{-/-}$ ESCs (Fig. 3E). Higher magnification further revealed the intense black staining in D3 when compared with HO-1$^{-/-}$ cells (Fig. 3F-G). Together, these results indicate that lack of HO-1 increases adipogenic but decreases osteogenic differentiation capacity, similar to the findings in MSCs by pharmacological manipulations [29].

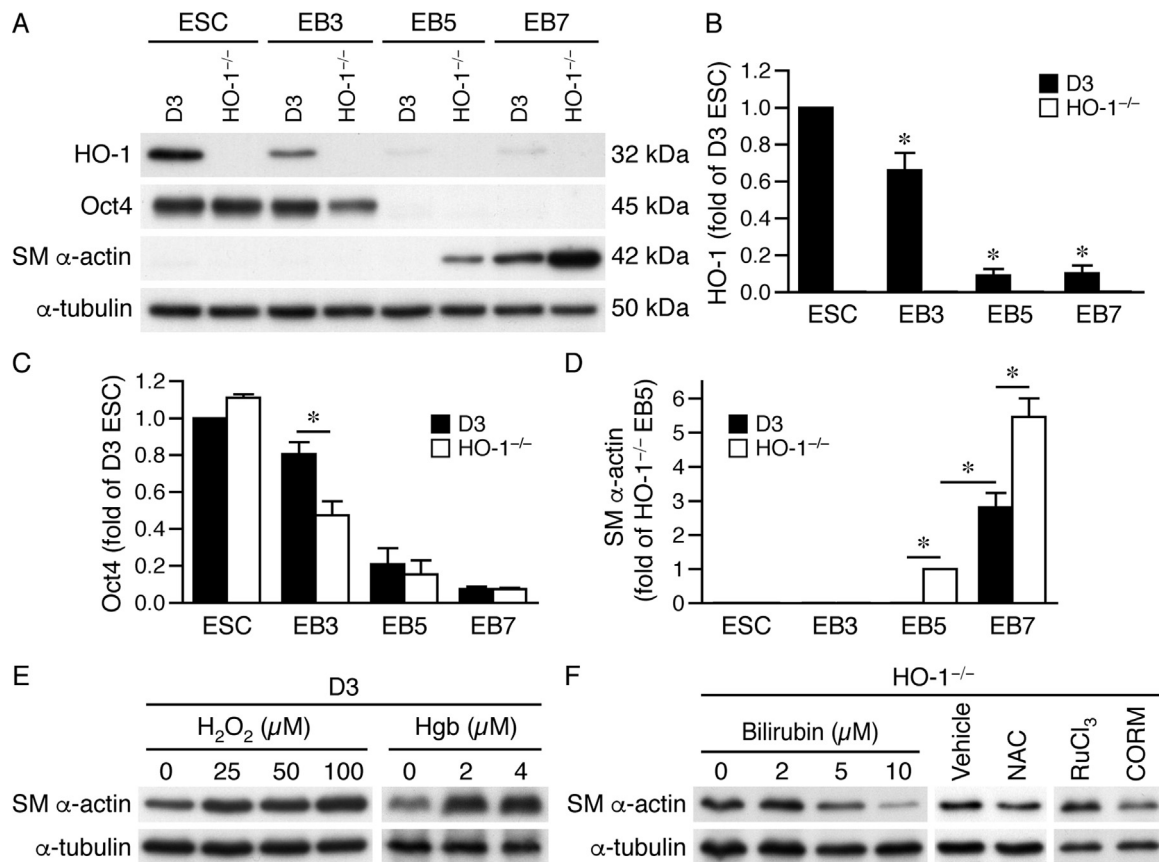### 3.5. Loss of HO-1 accelerates smooth muscle α-actin expression during EB development

Given that HO-1 exerts opposing effect on adipogenesis and osteogenesis, we wanted to further clarify the role of HO-1 in mesodermal differentiation. To this end, we examined another mesodermal lineage—smooth muscle cells (SMCs). SM α-actin is a major constituent of the contractile apparatus of SMCs in several organ systems, including vascular, respiratory and gastrointestinal systems, contributing to tissue structure and function. Therefore, we measured SM α-actin expression during EB differentiation. In the course of EB development, HO-1 expression level notably decreased to 0.66 ± 0.10-fold in 3-day D3 EBs (vs. ESC, $P < 0.05$) and further reduced to very low levels in 5- and 7-day EBs (0.09 ± 0.04 and 0.10 ± 0.04-fold, respectively; vs. ESC, $P < 0.05$). This pattern of HO-1 expression in EBs differed from that of

monolayer spontaneous differentiation, in which HO-1 was induced initially (Supplement Fig. S1). Nonetheless, modulation of HO-1 level indicated a role of HO-1 during EB development. HO-1 was not detectable in HO-1$^{-/-}$ EBs at all stages (Fig. 4A-B). The stem cell marker Oct4 decreased to 0.81 ± 0.07-fold (vs. ESC, $P < 0.05$) after 3 days (Fig. 4A, C). Compared with D3, loss of HO-1 resulted in an accelerated reduction of Oct4 to 0.48 ± 0.08-fold in 3-day EBs (Fig. 5A, C; vs. D3, $P < 0.05$). Oct4 further decreased to very low levels in 5- and 7-day EBs in both genotypes (Fig. 4A, C). As expected, SM α-actin was not detectable in ESCs or 3-day EBs (Fig. 4A). Interestingly, although SM α-actin was not detectable in 5-day D3 EBs it was notably expressed in 5-day HO-1$^{-/-}$ EBs (vs. D3, $P < 0.05$; Fig. 4A, D). Additional 2 days of EB development led to substantial SM α-actin expression in 7-day D3 EBs (2.82 ± 0.42 fold of 5-day HO-1$^{-/-}$EBs, $P < 0.05$), whereas HO-1 deficiency enhanced SM α-actin level to 5.46 ± 0.55 fold ($P < 0.05$, vs. 7-day D3; Fig. 4A, D).

To further confirm that loss of HO-1 enhances SMC differentiation, we examined another SMC maker SM22α. Both SM α-actin and SM22α contain CArG elements (CC(A/T)$_6$GG) in their genes for SMC-specific expressions. Western blot analysis revealed that as with SM α-actin, HO-1 deficiency increased SM22α in 5- and 7-day EBs in comparison with D3 (Fig. S4). These results suggest that lack of HO-1 accelerates and enhances SMC differentiation during EB development.

HO-1 deficiency promoted adipogenesis in directed differentiation (Fig. 3A-C) and enhanced SM α-actin expression during EB development (Fig. 4A, D); however, it was not clear whether loss of HO-1 rendered EB differentiation more prone to adipocytes or SMCs. We thus investigated the percentage differentiation of adipocytes and SMCs in 7-day D3 and HO-1$^{-/-}$ EBs. Nile red was used to stain for adipocytes and SM α-actin antibody for SMCs in flow cytometric assays. Interestingly, Nile red-positive cells were barely detectable (0.13 ± 0.07% and 0.04 ± 0.04% in D3 and HO-1$^{-/-}$, respectively) (Fig. S5A, B, E). In

Fig. 4. *Loss of HO-1 accelerates smooth muscle α-actin expression during EB development.* (A) D3 and HO-1$^{-/-}$ ESCs were subjected to 3-dimensional EB differentiation model and total proteins were isolated from ESCs and 3, 5, and 7 days after EB formation (EB3, EB5, and EB7, respectively). Western blot analysis was performed to detect HO-1, Oct4, and SM α-actin expressions. Blots were subsequently probed with α-tubulin for normalization. (B) Quantitative analysis of HO-1 in D3 and HO-1$^{-/-}$ ESC-EB system. The level in D3 ESCs was set as 1. Values are mean ± SE of 3 experiments. *$P < 0.05$ vs. ESC. (C) Quantitative analysis of Oct4 in D3 and HO-1$^{-/-}$ ESC-EB system. The level in D3 ESCs was set as 1. Values are mean ± SE of 3 experiments. *$P < 0.05$ vs. D3. (D) Quantitative analysis of SM α-actin in D3 and HO-1$^{-/-}$ ESC-EB system. Since SM α-actin was not expressed in ESCs and EB3, thus the level in HO-1$^{-/-}$ EB5 was set as 1. Values are mean ± SE of 3 experiments. *$P < 0.05$. (E) Three-day D3 EBs were treated with H_2O_2 (0, 25, 50, and 100 μM) to increase ROS or hemoglobin (0, 2, and 4 μM) to chelate CO. Proteins were isolated from 7-day EBs and Western blotting performed to detect SM α-actin. To verify equivalent loading, blots were probed with α-tubulin. At least 3 experiments were performed and a representative blot is shown. (F) HO-1$^{-/-}$ 3-day EBs were treated with bilirubin (0, 2, 5, and 10 μM), 1 mM NAC (vehicle H_2O), or CO-releasing molecule 50 μM CORM2 (RuCl$_3$ as a control compound). Proteins were isolated 2 days later for Western blotting to detect SM α-actin. Blots were subsequently probed with α-tubulin to verify loading. At least 3 experiments were performed and a representative blot is shown.

contrast, there were 26.6 ± 1.2% SM α-actin-positive cells in 7-day D3 EBs and loss of HO-1 increased the percentage to 45.8 ± 1.2% (Fig. S5C-E; vs. D3, $P < 0.05$). These results indicate that after 7 days in the EB differentiation model, there is significant SMC development while adipogenesis is minimal. These data further support the notion that deficiency of HO-1 enhanced SM α-actin expression and SMC development.

Because lack of HO-1 significantly enhanced ROS levels at day 3 during EB development (Fig. 2A), we tested whether elevated SM α-actin expression was due to increased oxidant level at the early time point. At day 3, we treated D3 EBs with increasing concentrations of H_2O_2 and harvested EBs at day 7 for Western analysis. Indeed, H_2O_2 increased SM α-actin proteins (Fig. 4E). One of the reaction products of HO-1 is CO, which has important physiological functions. Thus, we treated 3-day D3 EBs with different concentrations of hemoglobin to chelate CO. Interestingly, CO chelation also increased SM α-actin levels (Fig. 4E). We next performed rescue experiments by treating 3-day HO-1$^{-/-}$ EBs with bilirubin (one of the HO-1's reaction products and an antioxidant). Bilirubin dose-dependently reduced SM α-actin expression (Fig. 4F). To confirm the antioxidant effect of bilirubin, we used another antioxidant NAC to treat HO-1$^{-/-}$ EBs. As with bilirubin, NAC decreased SM α-actin level (Fig. 4F). Compared with control compound RuCl$_3$, exogenously adding CO releasing molecule CORM2 also decreased SM α-actin level (Fig. 4F). CO is well known for its anti-

inflammatory and anti-proliferative effects; however, the mechanisms by which CO affects SMC differentiation during EB development are unclear. Although CO can increase oxidative stress [50], a recent report showed that low concentrations of CO could reduce ROS generation, enhance intracellular glutathione and superoxide dismutase levels [51]. Therefore, it is possible that HO-1 deficiency resulted in a reduced CO concentration and further contributing to increases of ROS. Collectively, these data demonstrate that HO-1 exerts its effects via the reaction products and loss of HO-1 accelerates and enhances mesodermal SM α-actin expression during EB development.

3.6. Absence of HO-1 accelerates serum response factor and myocardin expression during EB development

The transcription factor SRF has been demonstrated to be an essential regulator of mesoderm formation by targeted gene deletion experiments [52,53]. Studies show that SRF binds to CArG element and mediates many smooth muscle-specific marker gene expressions [54]. However, SRF itself does not possess strong transcriptional activity and is not specifically expressed in SMCs. It was later discovered that myocardin, expressed specifically in smooth and cardiac muscles, is a potent transcriptional coactivator of SRF and strongly activates expressions of SMC marker genes, such as SM α-actin [55–57]. Loss of myocardin leads to early embryonic lethality and failure of mesoderm-
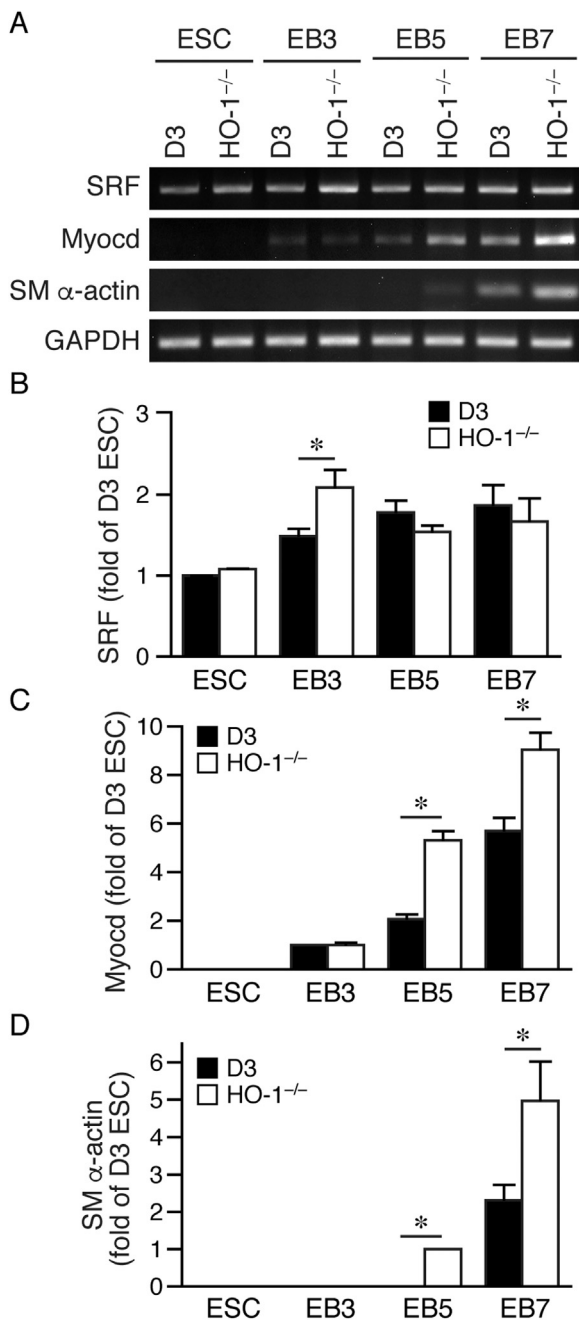
Fig. 5. *HO-1 deficiency accelerates* serum response factor *and myocardin expression during EB development.* (A) To examine SMC transcriptional regulators, total RNA was isolated from D3 and HO-1$^{-/-}$ ESC-EB system. RT-PCR was performed to amplify SRF and its coactivator myocardin. SM α-actin and GAPDH (for normalization) were also amplified. PCR products were analyzed on agarose gels and quantified using ImageJ. (B) SRF level in D3 ESCs was set as 1. Values are mean ± SE of 4 experiments. *P < 0.05 vs. D3. (C) Myocardin level in D3 EB3 was set as 1. Values are mean ± SE of 3 experiments. *P < 0.05 vs. D3. (D) SM α-actin level in HO-1$^{-/-}$ EB5 was set as 1. Values are mean ± SE of 4 experiments. *P < 0.05 vs. D3.

derived dorsal aortic SMC differentiation [58]. Thus, we examined SRF and myocardin expressions during EB development. RT-PCR analysis revealed that although SRF level increased following EB formation in both D3 and HO-1$^{-/-}$ cells (Fig. 5A-B), lack of HO-1 resulted in a significantly higher level of SRF in 3-day EBs (Fig. 5A-B). Myocardin was not expressed in ESCs but detectable in 3-day EBs, and increased to 2.1 ± 0.2 and 5.7 ± 0.6-fold (of D3-EB3) at 5- and 7-day D3 EBs, respectively (Fig. 5A, C). Compared with D3, myocardin was significantly elevated in HO-1$^{-/-}$ 5- and 7-day EBs (5.30 ± 0.4 and 9.0 ± 0.7-fold,

respectively). The greatest difference was observed in EB5, 5.3 ± 0.4 vs. 2.1 ± 0.2-fold of D3 (Fig. 5A, C). SM α-actin was detectable after 5 days in HO-1$^{-/-}$ but not D3 EBs (Fig. 5A, D). When SM α-actin of HO-1$^{-/-}$ EB5 was set as 1, loss of HO-1 substantially increased SM α-actin expression in EB7 to 5.0 ± 1.1-fold compared with 2.3 ± 0.4-fold of D3 (Fig. 5A, D). The greatest difference of SM α-actin expression between D3 and HO-1$^{-/-}$ EBs occurred at day 5, which coincided with that of myocardin. Taken together, our results suggest that absence of HO-1 accelerates induction of SRF at day 3 and its coactivator myocardin at day 5, leading to accelerated and enhanced expression of SM α-actin.

3.7. Smad2 in pluripotency and SMC differentiation

TGFβ/Activin signaling is crucial for the self-renewal and pluripotency of human ESCs [59]. The downstream effectors Smad2/3 participate in the signaling switch that controls self-renewal and differentiation [60]. Further, Smad2, but not Smad3, is essential for the maintenance of pluripotency in human ESCs and mouse epiblast stem cells [61]. In contrast to human ESCs, Smad2 is not required for self-renewal of mouse ESCs downstream of Activin/Nodal signaling [62]. Intriguingly, Smad2/3 mediates, at least in part, TGFβ-induced SMC marker gene expressions, such as SM α-actin [63,64] and contributes to SMC differentiation [65]. To determine whether Smad2 contributes to HO-1-mediated SM α-actin expression during EB development, we examined Smad2 levels in ESC-EB system in the presence or absence of HO-1. Western blotting revealed that Smad2 level was significantly higher in HO-1$^{-/-}$ than D3 ESCs (Fig. 6A-B). Smad2 expression was downregulated following EB formation at day 3 in both genotypes and then gradually increased thereafter at 5 and 7 days (Fig. 6A-B). Interestingly, HO-1$^{-/-}$ EBs maintained a significantly higher level of Smad2 than D3 at 3 and 5 days, and had enhanced expression of SM α-actin at day 5 and 7 (Fig. 6A-C). This pattern of expression suggests that higher levels of Smad2 in HO-1$^{-/-}$ ESC-EB are associated with accelerated and higher expression of SM α-actin in HO-1$^{-/-}$ than D3 EBs (Fig. 6A-C). In addition to Smad2, Erk1/2 signaling cascade has been shown to trigger transition of pluripotent ESCs from self-renewal to lineage commitment [66], we thus examined Erk1/2 activation in our EB system. Similar to Smad2, phospho-Erk1/2 was higher in HO-1$^{-/-}$ than D3 ESCs and downregulated following EB formation at day 3 in both genotypes and then gradually increased thereafter at 5 and 7 days (Fig. 6D). Intriguingly, compared with D3, phospho-Erk1/2 levels were higher in HO-1$^{-/-}$ EBs at 5 and 7 days (Fig. 6D). These data suggest that an absence of HO-1 elevates phospho-Erk1/2 levels during EB differentiation, which in combination with increased Smad2 might contribute to enhanced mesodermal maturation.

To determine whether HO-1 regulates Smad2 expression, we knocked down HO-1 level in D3 ESCs by siRNA. Western analysis showed that compared with control siRNA, transfection of HO-1 siRNA reduced HO-1 level to 0.62 ± 0.07-fold of control (P < 0.005, n = 3) and increased Smad2 expression to 1.15 ± 0.01-fold (P < 0.005 vs. siControl, n = 3; Fig. 6D). Conversely, transfecting HO-1$^{-/-}$ ESCs with HO-1 expression plasmid resulted in re-expression of HO-1 when compared with vector control (Fig. 6E), and reduced Smad2 level to 0.80 ± 0.07 fold (P < 0.005 vs. vector, n = 4; Fig. 6F). Together, these results indicate that loss of HO-1 in ESCs enhances Smad2 expression, contributing at least in part to accelerated and higher expression of SM α-actin.

4. Discussion

HO-1 is well known to protect cells and tissues from injury. Our previous study shows that loss of HO-1 renders iPS cells more prone to lose pluripotency and more sensitive to oxidant stress-induced cell death [37]. However, the function of HO-1 in ESC differentiation is largely unclear. In the present study, we established mouse HO-1$^{-/-}$ ESC lines and used these cells to investigate the role of HO-1 during ESC
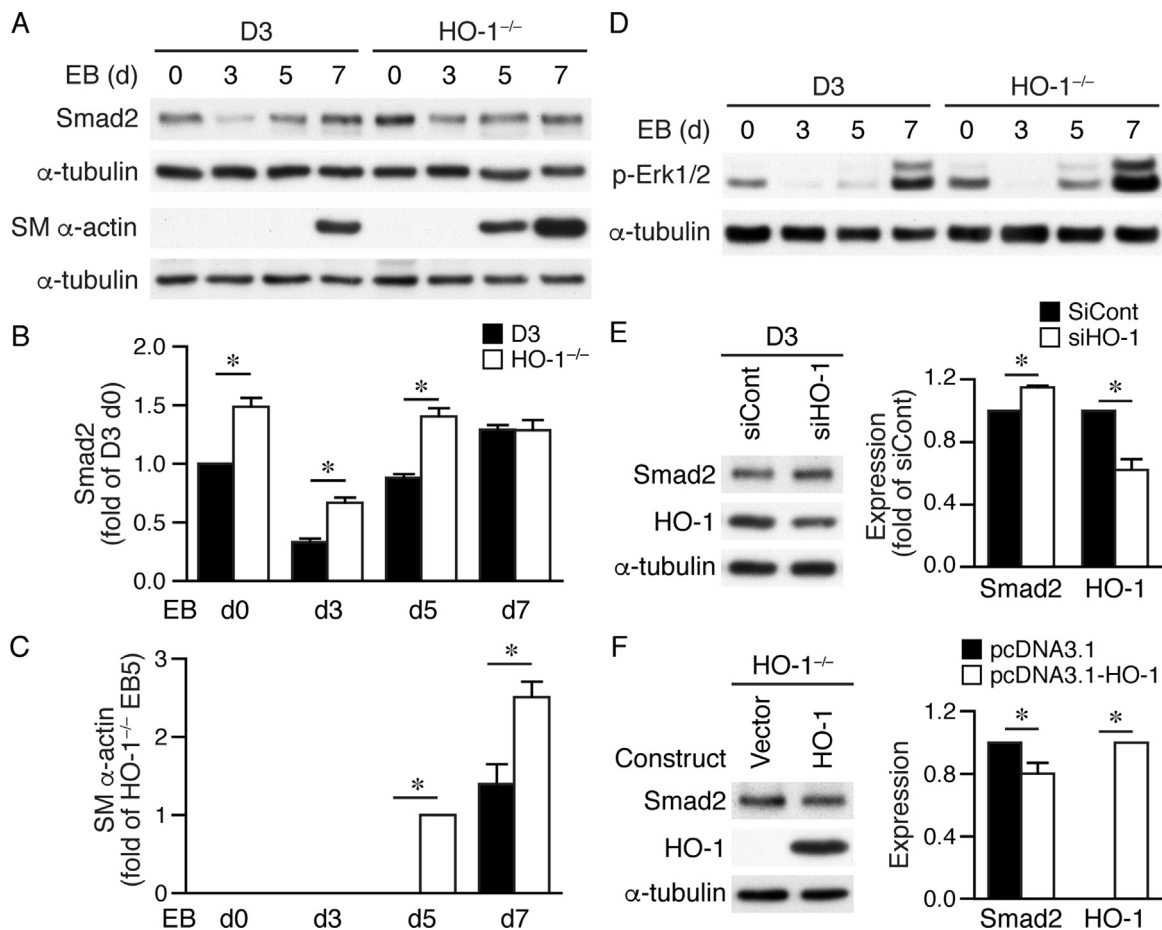
Fig. 6. *HO-1 regulates Smad2 expression and SMC differentiation.* Total proteins were isolated from D3 and HO-1$^{-/-}$ ESC-EB system and Western blotting performed to analyze Smad2 and SM α-actin expressions. Blots were subsequently probed with α-tubulin for normalization. (B) Smad2 level in D3 ESCs (d0) was set as 1. Values are mean ± SE of 3 experiments. *$P < 0.05$ vs. D3. (C) SM α-actin level in HO-1$^{-/-}$ EB5 (d5) was set as 1. Values are mean ± SE of 3 experiments. *$P < 0.05$ vs. D3. (D) Western blot analysis was performed to detect Erk1/2 phosphorylation. To verify equal loading, blots were subsequently probed with α-tubulin for normalization. A representative of 3 experiments is shown. (E) D3 ESCs were transfected with control (siCont) or HO-1 siRNA (siHO-1) and cultured in ESC medium. Left panel: Proteins were harvested for Western blotting 2 days later to detect Smad2 and HO-1, and α-tubulin for normalization. Right panel: Smad2 and HO-1 level of siControl was set as 1. Values are mean ± SE of 3 experiments. *$P < 0.05$ vs. siCont. (F) HO-1$^{-/-}$ ESCs were transfected with control vector pcDNA3.1 or HO-1 expression plasmid pcDNA3.1-HO-1 and cultured in ESC medium. Left panel: Proteins were harvested for Western blotting 2 days later to detect Smad2 and HO-1, and α-tubulin for normalization. At least 3 experiments were performed and a representative blot is shown. Right panel: Smad2 and HO-1 level of vector control was set as 1. Values are mean ± SE of 3 experiments. *$P < 0.05$ vs. pcDNA3.1 vector.

differentiation. We showed that loss of HO-1 led to enhanced ROS level, concomitant with increased expressions of mesendodermal and SMC regulators. Concerted actions of SMC regulators and Smad2 resulted in accelerated and enhanced SM α-actin expression in HO-1$^{-/-}$ EBs following differentiation. Our results reveal a previously unrecognized critical role of HO-1 in regulating SMC gene expressions during ESC-EB development.

Given that ESCs are characterized by low ROS level [33], it is not surprising that HO-1 is not required for maintaining pluripotency. As such, we were able to establish HO-1$^{-/-}$ ESCs displaying pluripotent markers (Fig. 1). On the other hand, numerous studies have shown that the processes of differentiation increase ROS levels, which serve as signaling molecules for differentiation [35,47]. Indeed, ROS level progressively increased in D3 during EB development (Fig. 2A). Correlating with increased ROS level, HO-1 expression was downregulated in D3 in the course of EB development (Fig. 4A-B), implicating involvement of HO-1 in modulating ROS level. In support of this notion, we found that compared with D3, loss of the antioxidative HO-1 resulted in enhanced ROS level at the early 3-day time point during EB development (Fig. 2A). In parallel, mesendodermal transcription factors were significantly upregulated (Fig. 2B-C). In particular, there was a robust surge of the mesodermal master regulator brachyury (Fig. 2C), which is essential for mesoderm but not for endoderm formation [67].

Intriguingly, brachyury protein was detectable mainly at day 3 in both D3 and HO-1$^{-/-}$ EBs (Fig. 2E). Brachyury expression occurs in early stage mesoderm, and the period of high-level expression of brachyury in HO-1$^{-/-}$ cells coincides with the time of mesoderm formation [48,49]. Intriguingly, the robust expression of brachyury corresponded with upregulation of SRF at day 3 (Fig. 5A-B). The importance of SRF in contributing to mesodermal gene expressions of ESCs has been demonstrated using SRF$^{-/-}$ ESCs, which display a defect in mesodermal differentiation [53]. Moreover, binding of SRF to CArG element is a critical step in activating SMC-specific gene expressions [65,68]. Following SRF elevation, lack of HO-1 enhanced expression of myocardin, a strong transcriptional coactivator of SRF and a key component of a molecular switch for SMC differentiation [55] (Fig. 5A, C). The collective induction of regulators that control SMC gene expressions are likely to contribute to accelerated and enhanced SMC gene expressions of HO-1$^{-/-}$ EBs (Fig. 4A, D).

Compared with D3 ESCs, HO-1$^{-/-}$ ESCs had higher level of Smad2, suggesting a role of HO-1 in suppressing Smad2 expression in ESCs. This notion was supported by that knocking down HO-1 level in D3 ESCs with siRNA increased Smad2 whereas re-expression of HO-1 in HO-1$^{-/-}$ ESCs decreased Smad2 level (Fig. 6). Although Smad2 is critical for human ESC pluripotency downstream of TGFβ/Activin signaling [59,60,69], Smad2 is dispensable for self-renewal maintenance

of mouse ESCs [62]. Supporting this view, we found that higher level of Smad2 in HO-1$^{-/-}$ ESCs did not alter ESC characteristics, including short doubling time and stemness markers. Despite that Smad2 is not required for the maintenance of pluripotency, Smad2 is essential for proper lineage commitment, especially of mesendoderm [62]. Decreasing Smad2 expression results in loss of pluripotent gene expressions and an increased expression of brachyury [61]. In line with this, we found that in D3, there was a reduction of Smad2 and an increase of brachyury following differentiation—after 3 days of EB formation (Figs. 2 and 6). Although similar to D3, there was a reduction of Smad2 in HO-1$^{-/-}$ 3-day EB from day 0, its level was higher than that in D3 (Fig. 6A-B). Intriguingly, higher level of Smad2 in HO-1$^{-/-}$ 3-day EB correlated with the robust induction of brachyury (Fig. 2C). It is tempting to speculate that although higher level of Smad2 in HO-1$^{-/-}$ ESCs did not affect pluripotency, it rendered HO-1$^{-/-}$ ESCs more prone to differentiate toward mesodermal lineage when a differentiation cue is present. It is likely that higher level of Smad2 caused an exaggerated induction of brachyury at the critical early time point. Alternatively, robust induction of brachyury might be the result of enhanced ROS level due to loss of HO-1.

A role of Smad2 in SMC differentiation has been well established. TGFβ signaling through Smad2/3 contributes to the development of SMCs from mouse ESCs in differentiation studies [70]. Furthermore, Smad2/3 mediates, at least in part, TGFβ-induced SMC marker gene expressions, including SM α-actin [63,64] and contributes to SMC differentiation [65]. In agreement with this concept, the return of Smad2 level at later time points might be important for SMC gene expressions (Fig. 6). Further supporting this view, it has been shown in human ESCs that brachyury interacts and collaborates with Smad2/3 signaling to regulate the expression of its target genes in a cell-specific manner [67]. As such, Smad2 and brachyury, together with SMC regulators SRF and myocardin, might orchestrate in a coordinate manner to drive SMC gene expressions. In addition, Erk1/2 signaling cascade has been shown to trigger transition of pluripotent ESCs from self-renewal to lineage commitment [66]. Indeed, compared with D3, Erk1/2 activation was enhanced in 7-day HO-1$^{-/-}$ EBs, suggesting Erk1/2 may also participate in regulating mesoderm SMC differentiation.

In conclusion, using HO-1$^{-/-}$ ESCs rather than iPS cells, we demonstrated that HO-1 is not required for self-renewal and pluripotency of mouse ESCs; instead, HO-1 plays a critical role in modulating mesodermal SMC expressions during differentiation. HO-1 might exert its effect during differentiation through regulating ROS level and subsequent modulations of mesodermal/SMC transcriptional regulators. More importantly, our findings may provide a novel strategy in directing ESC differentiation toward SMC lineage. In addition, organoids derived from HO-1$^{-/-}$ ESCs might provide a platform for therapeutic drug screening for HO-1 deficiency-related diseases.

Acknowledgments

Declaration of interest

The authors declare that they have no competing interests.

Appendix A. Supporting information

Supplementary data associated with this article can be found in the online version at http://dx.doi.org/10.1016/j.redox.2017.11.019.

References

[1] M.D. Maines, The heme oxygenase system: a regulator of second messenger gases, Annu. Rev. Pharmacol. Toxicol. 37 (1997) 517–554.

[2] R.S. Eisenstein, D. Garcia-Mayol, W. Pettingell, H.N. Munro, Regulation of ferritin and heme oxygenase synthesis in rat fibroblasts by different forms of iron, Proc. Natl. Acad. Sci. USA 88 (1991) 688–692.

[3] R. Stocker, Y. Yamamoto, A.F. McDonagh, A.N. Glazer, B.N. Ames, Bilirubin is an antioxidant of possible physiological importance, Science 235 (1987) 1043–1046.

[4] L.E. Otterbein, L.L. Mantell, A.M. Choi, Carbon monoxide provides protection against hyperoxic lung injury, Am. J. Physiol. 276 (1999) L688–L694.

[5] L.E. Otterbein, F.H. Bach, J. Alam, M. Soares, H. Tao Lu, M. Wysk, R.J. Davis, R.A. Flavell, A.M. Choi, Carbon monoxide has anti-inflammatory effects involving the mitogen-activated protein kinase pathway, Nat. Med. 6 (2000) 422–428.

[6] K.D. Poss, S. Tonegawa, Reduced stress defense in heme oxygenase 1-deficient cells, Proc. Natl. Acad. Sci. USA 94 (1997) 10925–10930.

[7] S.W. Ryter, J. Alam, A.M. Choi, Heme oxygenase-1/carbon monoxide: from basic science to therapeutic applications, Physiol. Rev. 86 (2006) 583–650.

[8] A. Loboda, M. Damulewicz, E. Pyza, A. Jozkowicz, J. Dulak, Role of Nrf2/HO-1 system in development, oxidative stress response and diseases: an evolutionarily conserved mechanism, Cell. Mol. Life Sci. 73 (2016) 3221–3247.

[9] S.F. Yet, M.A. Perrella, M.D. Layne, C.M. Hsieh, K. Maemura, L. Kobzik, P. Wiesel, H. Christou, S. Kourembanas, M.E. Lee, Hypoxia induces severe right ventricular dilatation and infarction in heme oxygenase-1 null mice, J. Clin. Investig. 103 (1999) R23–R29.

[10] S.F. Yet, R. Tian, M.D. Layne, Z.Y. Wang, K. Maemura, M. Solovyeva, B. Ith, L.G. Melo, L. Zhang, J.S. Ingwall, V.J. Dzau, M.E. Lee, M.A. Perrella, Cardiac-specific expression of heme oxygenase-1 protects against ischemia and reperfusion injury in transgenic mice, Circ. Res. 89 (2001) 168–173.

[11] M. Katori, R. Buelow, B. Ke, J. Ma, A.J. Coito, S. Iyer, D. Southard, R.W. Busuttil, J.W. Kupiec-Weglinski, Heme oxygenase-1 overexpression protects rat hearts from cold ischemia/reperfusion injury via an antiapoptotic pathway, Transplantation 73 (2002) 287–292.

[12] L.G. Melo, R. Agrawal, L. Zhang, M. Rezvani, A.A. Mangi, A. Ehsan, D.P. Griese, G. Dell'Acqua, M.J. Mann, J. Oyama, S.F. Yet, M.D. Layne, M.A. Perrella, V.J. Dzau, Gene therapy strategy for long-term myocardial protection using adeno-associated virus-mediated delivery of heme oxygenase gene, Circulation 105 (2002) 602–607.

[13] X. Liu, J. Wei, D.H. Peng, M.D. Layne, S.F. Yet, Absence of heme oxygenase-1 exacerbates myocardial ischemia/reperfusion injury in diabetic mice, Diabetes 54 (2005) 778–784.

[14] H.J. Duckers, M. Boehm, A.L. True, S.F. Yet, H. San, J.L. Park, R. Clinton Webb, M.E. Lee, G.J. Nabel, E.G. Nabel, Heme oxygenase-1 protects against vascular constriction and proliferation, Nat. Med. 7 (2001) 693–698.

[15] S.F. Yet, M.D. Layne, X. Liu, Y.H. Chen, B. Ith, N.E. Sibinga, M.A. Perrella, Absence of heme oxygenase-1 exacerbates atherosclerotic lesion formation and vascular remodeling, FASEB J. 17 (2003) 1759–1761.

[16] B.J. Wu, K. Kathir, P.K. Witting, K. Beck, K. Choy, C. Li, K.D. Croft, T.A. Mori, D. Tanous, M.R. Adams, A.K. Lau, R. Stocker, Antioxidants protect from atherosclerosis by a heme oxygenase-1 pathway that is independent of free radical scavenging, J. Exp. Med. 203 (2006) 1117–1127.

[17] Y.C. Ho, M.L. Wu, P.Y. Gung, C.H. Chen, C.C. Kuo, S.F. Yet, Heme oxygenase-1 deficiency exacerbates angiotensin II-induced aortic aneurysm in mice, Oncotarget 7 (2016) 67760–67776.

[18] M.L. Wu, Y.C. Ho, S.F. Yet, A central role of heme oxygenase-1 in cardiovascular protection, Antioxid. Redox Signal. 15 (2011) 1835–1846.

[19] Y.M. Kim, H.O. Pae, J.E. Park, Y.C. Lee, J.M. Woo, N.H. Kim, Y.K. Choi, B.S. Lee, S.R. Kim, H.T. Chung, Heme oxygenase in the regulation of vascular biology: from molecular mechanisms to therapeutic opportunities, Antioxid. Redox Signal. 14 (2011) 137–167.

[20] L.E. Fredenburgh, A.A. Merz, S. Cheng, Haeme oxygenase signalling pathway: implications for cardiovascular disease, Eur. Heart J. 36 (2015) 1512–1518.

[21] M. Chang, J. Xue, V. Sharma, A. Habtezion, Protective role of hemeoxygenase-1 in gastrointestinal diseases, Cell. Mol. Life Sci. 72 (2015) 1161–1173.

[22] A. Yachie, Y. Niida, T. Wada, N. Igarashi, H. Kaneda, T. Toma, K. Ohta, Y. Kasahara, S. Koizumi, Oxidative stress causes enhanced endothelial cell injury in human heme oxygenase-1 deficiency, J. Clin. Investig. 103 (1999) 129–135.

[23] A. Kawashima, Y. Oda, A. Yachie, S. Koizumi, I. Nakanishi, Heme oxygenase-1 deficiency: the first autopsy case, Hum. Pathol. 33 (2002) 125–130.

[24] S. Koizumi, Human heme oxygenase-1 deficiency: a lesson on serendipity in the discovery of the novel disease, Pediatr. Int. 49 (2007) 125–132.

[25] N. Radhakrishnan, S.P. Yadav, A. Sachdeva, P.K. Pruthi, S. Sawhney, T. Piplani, T. Wada, A. Yachie, Human heme oxygenase-1 deficiency presenting with hemolysis, nephritis, and asplenia, J. Pediatr. Hematol. Oncol. 33 (2011) 74–78.

[26] M. Kozakowska, K. Szade, J. Dulak, A. Jozkowicz, Role of heme oxygenase-1 in postnatal differentiation of stem cells: a possible cross-talk with microRNAs, Antioxid. Redox Signal. 20 (2014) 1827–1850.

[27] S. Toobiak, M. Shaklai, N. Shaklai, Carbon monoxide induced erythroid differentiation of K562 cells mimics the central macrophage milieu in erythroblastic islands, PLoS One 7 (2012) e33940.

[28] B. Wegiel, A. Hedblom, M. Li, D. Gallo, E. Csizmadia, C. Harris, Z. Nemeth, B.S. Zuckerbraun, M. Soares, J.L. Persson, L.E. Otterbein, Heme oxygenase-1 derived carbon monoxide permits maturation of myeloid cells, Cell Death Dis. 5 (2014) e1139.

[29] L. Vanella, D.H. Kim, D. Asprinio, S.J. Peterson, I. Barbagallo, A. Vanella, D. Goldstein, S. Ikehara, A. Kappas, N.G. Abraham, HO-1 expression increases mesenchymal stem cell-derived osteoblasts but decreases adipocyte lineage, Bone 46 (2010) 236–243.

[30] G. Wagner, J. Lindroos-Christensen, E. Einwallner, J. Husa, T.C. Zapf, K. Lipp, S. Rauscher, M. Groger, A. Spittler, R. Loewe, F. Gruber, J.C. Duvigneau, T. Mohr, H. Sutterluty-Fall, F. Klinglmuller, G. Prager, B. Huppertz, J. Yun, O. Wagner, H. Esterbauer, M. Bilban, HO-1 inhibits preadipocyte proliferation and differentiation at the onset of obesity via ROS dependent activation of Akt2, Sci. Rep. 7 (2017) 40881.

[31] K.D. Poss, S. Tonegawa, Heme oxygenase 1 is required for mammalian iron reutilization, Proc. Natl. Acad. Sci. USA 94 (1997) 10919–10924.

[32] K. Wang, T. Zhang, Q. Dong, E.C. Nice, C. Huang, Y. Wei, Redox homeostasis: the linchpin in stem cell self-renewal and differentiation, Cell Death Dis. 4 (2013) e537.

[33] O.G. Lyublinskaya, J.S. Ivanova, N.A. Pugovkina, I.V. Kozhukharova, Z.V. Kovaleva, A.N. Shatrova, N.D. Aksenov, V.V. Zenin, Y.A. Kaulin, I.A. Gamaley, N.N. Nikolsky, Redox environment in stem and differentiated cells: a quantitative approach, Redox Biol. 12 (2017) 758–769.

[34] H. Sauer, G. Rahimi, J. Hescheler, M. Wartenberg, Role of reactive oxygen species and phosphatidylinositol 3-kinase in cardiomyocyte differentiation of embryonic stem cells, FEBS Lett. 476 (2000) 218–223.

[35] G. Saretzki, T. Walter, S. Atkinson, J.F. Passos, B. Bareth, W.N. Keith, R. Stewart, S. Hoare, M. Stojkovic, L. Armstrong, T. von Zglinicki, M. Lako, Downregulation of multiple stress defense mechanisms during differentiation of human embryonic stem cells, Stem Cells 26 (2008) 455–464.

[36] W.L. Trigona, C.M. Porter, J.A. Horvath-Arcidiacono, A.S. Majumdar, E.T. Bloom, Could heme-oxygenase-1 have a role in modulating the recipient immune response to embryonic stem cells? Antioxid. Redox Signal. 9 (2007) 751–756.

[37] C.Y. Lin, C.Y. Peng, T.T. Huang, M.L. Wu, Y.L. Lai, D.H. Peng, P.F. Chen, H.F. Chen, B.L. Yen, K.K. Wu, S.F. Yet, Exacerbation of oxidative stress-induced cell death and differentiation in induced pluripotent stem cells lacking heme oxygenase-1, Stem Cells Dev. 21 (2012) 1675–1687.

[38] M.H. Chin, M.J. Mason, W. Xie, S. Volinia, M. Singer, C. Peterson, G. Ambartsumyan, O. Aimiuwu, L. Richter, J. Zhang, I. Khvorostov, V. Ott, M. Grunstein, N. Lavon, N. Benvenisty, C.M. Croce, A.T. Clark, T. Baxter, A.D. Pyle, M.A. Teitell, M. Pelegrini, K. Plath, W.E. Lowry, Induced pluripotent stem cells and embryonic stem cells are distinguished by gene expression signatures, Cell Stem Cell 5 (2009) 111–123.

[39] B.Y. Hu, J.P. Weick, J. Yu, L.X. Ma, X.Q. Zhang, J.A. Thomson, S.C. Zhang, Neural differentiation of human induced pluripotent stem cells follows developmental principles but with variable potency, Proc. Natl. Acad. Sci. USA 107 (2010) 4335–4340.

[40] K.H. Lee, C.K. Chuang, S.F. Guo, C.F. Tu, Simple and efficient derivation of mouse embryonic stem cell lines using differentiation inhibitors or proliferation stimulators, Stem Cells Dev. 21 (2012) 373–383.

[41] A. Bishop, S.F. Yet, M.E. Lee, M.A. Perrella, B. Demple, A key role for heme oxygenase-1 in nitric oxide resistance in murine motor neurons and glia, Biochem. Biophys. Res. Commun. 325 (2004) 3–9.

[42] G. Saretzki, L. Armstrong, A. Leake, M. Lako, T. von Zglinicki, Stress defense in murine embryonic stem cells is superior to that of various differentiated murine cells, Stem Cells 22 (2004) 962–971.

[43] N.L. Woll, S.K. Bronson, Analysis of embryonic stem cell-derived osteogenic cultures, Methods Mol. Biol. 330 (2006) 149–159.

[44] H. Ding, K.C. Keller, I.K. Martinez, R.M. Geransar, K.O. zur Nieden, S.G. Nishikawa, D.E. Rancourt, N.I. zur Nieden, NO-beta-catenin crosstalk modulates primitive streak formation prior to embryonic stem cell osteogenic differentiation, J. Cell Sci. 125 (2012) 5564–5577.

[45] K. Schaedlich, J.M. Knelangen, A. Navarrete Santos, B. Fischer, A. Navarrete Santos, A simple method to sort ESC-derived adipocytes, Cytom. Part A. 77 (2010) 990–995.

[46] A. Leahy, J.W. Xiong, F. Kuhnert, H. Stuhlmann, Use of developmental marker genes to define temporal and spatial patterns of differentiation during embryoid body formation, J. Exp. Zool. 284 (1999) 67–81.

[47] H. Sauer, M. Wartenberg, Reactive oxygen species as signaling molecules in cardiovascular differentiation of embryonic stem cells and tumor-induced angiogenesis, Antioxid. Redox Signal. 7 (2005) 1423–1434.

[48] D.G. Wilkinson, S. Bhatt, B.G. Herrmann, Expression pattern of the mouse T gene and its role in mesoderm formation, Nature 343 (1990) 657–659.

[49] M. Lolas, P.D. Valenzuela, R. Tjian, Z. Liu, Charting Brachyury-mediated developmental pathways during early mouse embryogenesis, Proc. Natl. Acad. Sci. USA 111 (2014) 4478–4483.

[50] C. Reboul, J. Boissiere, L. Andre, G. Meyer, P. Bideaux, G. Fouret, C. Feillet-Coudray, P. Obert, A. Lacampagne, J. Thireau, O. Cazorla, S. Richard, Carbon monoxide pollution aggravates ischemic heart failure through oxidative stress pathway, Sci. Rep. 7 (2017) 39715.

[51] Y. Huang, T. Ma, Z. Ye, H. Li, Y. Zhao, W. Chen, Y. Fu, Z. Ye, A. Sun, Z. Li, Carbon monoxide (CO) inhibits hydrogen peroxide (H$_2$O$_2$)-induced oxidative stress and the activation of NF-kappaB signaling in lens epithelial cells, Exp. Eye Res. 166 (2017) 29–39.

[52] S. Arsenian, B. Weinhold, M. Oelgeschlager, U. Ruther, A. Nordheim, Serum response factor is essential for mesoderm formation during mouse embryogenesis, EMBO J. 17 (1998) 6289–6299.

[53] B. Weinhold, G. Schratt, S. Arsenian, J. Berger, K. Kamino, H. Schwarz, U. Ruther, A. Nordheim, Srf$^{-/-}$ ES cells display non-cell-autonomous impairment in mesodermal differentiation, EMBO J. 19 (2000) 5835–5844.

[54] T. Yoshida, G.K. Owens, Molecular determinants of vascular smooth muscle cell diversity, Circ. Res. 96 (2005) 280–291.

[55] J. Chen, C.M. Kitchen, J.W. Streb, J.M. Miano, Myocardin: a component of a molecular switch for smooth muscle differentiation, J. Mol. Cell. Cardiol. 34 (2002) 1345–1356.

[56] T. Yoshida, S. Sinha, F. Dandre, B.R. Wamhoff, M.H. Hoofnagle, B.E. Kremer, D.Z. Wang, E.N. Olson, G.K. Owens, Myocardin is a key regulator of CArG-dependent transcription of multiple smooth muscle marker genes, Circ. Res. 92 (2003) 856–864.

[57] K.L. Du, H.S. Ip, J. Li, M. Chen, F. Dandre, W. Yu, M.M. Lu, G.K. Owens, M.S. Parmacek, Myocardin is a critical serum response factor cofactor in the transcriptional program regulating smooth muscle cell differentiation, Mol. Cell. Biol. 23 (2003) 2425–2437.

[58] S. Li, D.Z. Wang, Z. Wang, J.A. Richardson, E.N. Olson, The serum response factor coactivator myocardin is required for vascular smooth muscle development, Proc. Natl. Acad. Sci. USA 100 (2003) 9366–9370.

[59] G.M. Beattie, A.D. Lopez, N. Bucay, A. Hinton, M.T. Firpo, C.C. King, A. Hayek, Activin A maintains pluripotency of human embryonic stem cells in the absence of feeder layers, Stem Cells 23 (2005) 489–495.

[60] A.M. Singh, D. Reynolds, T. Cliff, S. Ohtsuka, A.L. Mattheyses, Y. Sun, L. Menendez, M. Kulik, S. Dalton, Signaling network crosstalk in human pluripotent cells: a Smad2/3-regulated switch that controls the balance between self-renewal and differentiation, Cell Stem Cell 10 (2012) 312–326.

[61] M. Sakaki-Yumoto, J. Liu, M. Ramalho-Santos, N. Yoshida, R. Derynck, Smad2 is essential for maintenance of the human and mouse primed pluripotent stem cell state, J. Biol. Chem. 288 (2013) 18546–18560.

[62] T. Fei, S. Zhu, K. Xia, J. Zhang, Z. Li, J.D. Han, Y.G. Chen, Smad2 mediates Activin/Nodal signaling in mesendoderm differentiation of mouse embryonic stem cells, Cell Res. 20 (2010) 1306–1318.

[63] S. Chen, M. Kulik, R.J. Lechleider, Smad proteins regulate transcriptional induction of the SM22alpha gene by TGF-beta, Nucleic Acids Res. 31 (2003) 1302–1310.

[64] M.L. Wu, C.H. Chen, Y.T. Lin, Y.J. Jheng, Y.C. Ho, L.T. Yang, L. Chen, M.D. Layne, S.F. Yet, Divergent signaling pathways cooperatively regulate TGFβ induction of cysteine-rich protein 2 in vascular smooth muscle cells, Cell Commun. Signal. 12 (2014) 22.

[65] C.P. Mack, Signaling mechanisms that regulate smooth muscle cell differentiation, Arterioscler. Thromb. Vasc. Biol. 31 (2011) 1495–1505.

[66] T. Kunath, M.K. Saba-El-Leil, M. Almousailleakh, J. Wray, S. Meloche, A. Smith, FGF stimulation of the Erk1/2 signalling cascade triggers transition of pluripotent embryonic stem cells from self-renewal to lineage commitment, Development 134 (2007) 2895–2902.

[67] T. Faial, A.S. Bernardo, S. Mendjan, E. Diamanti, D. Ortmann, G.E. Gentsch, V.L. Mascetti, M.W. Trotter, J.C. Smith, R.A. Pedersen, Brachyury and SMAD signalling collaboratively orchestrate distinct mesoderm and endoderm gene regulatory networks in differentiating human embryonic stem cells, Development 142 (2015) 2121–2135.

[68] J.M. Miano, Serum response factor: toggling between disparate programs of gene expression, J. Mol. Cell. Cardiol. 35 (2003) 577–593.

[69] R.H. Xu, T.L. Sampsell-Barron, F. Gu, S. Root, R.M. Peck, G. Pan, J. Yu, J. Antosiewicz-Bourget, S. Tian, R. Stewart, J.A. Thomson, NANOG is a direct target of TGFbeta/activin-mediated SMAD signaling in human ESCs, Cell Stem Cell 3 (2008) 196–206.

[70] S. Sinha, M.H. Hoofnagle, P.A. Kingston, M.E. McCanna, G.K. Owens, Transforming growth factor-β1 signaling contributes to development of smooth muscle cells from embryonic stem cells, Am. J. Physiol. Cell Physiol. 287 (2004) C1560–C1568.